

# Magnetic and electrical transport behavior in the crystallographically disordered compound $U_2CoSi_3$

Maria Szlawska, Daniel Gnida, and Dariusz Kaczorowski\*

*Institute of Low Temperature and Structure Research, Polish Academy of Sciences, P. O. Box 1410, 50-950 Wrocław, Poland*

(Received 18 February 2011; revised manuscript received 26 July 2011; published 11 October 2011)

A single crystal of the uranium-based ternary silicide  $U_2CoSi_3$  has been investigated by means of magnetic, heat capacity, and electrical resistivity measurements, performed in wide ranges of the temperature and magnetic field. The compound crystallizes with a hexagonal  $AlB_2$ -type structure with crystallographic disorder in the nonmagnetic atom sublattice. The results indicate the formation at low temperatures of a ferromagnetic cluster-glass state, which likely originates from crystallographic disorder in the nonmagnetic atom sublattice of the hexagonal  $AlB_2$ -type unit cell. The low-temperature behavior of the electrical resistivity of  $U_2CoSi_3$  can be adequately described in terms of theories developed for disordered systems.

DOI: [10.1103/PhysRevB.84.134410](https://doi.org/10.1103/PhysRevB.84.134410)

PACS number(s): 75.50.Lk, 72.15.Rn

## I. INTRODUCTION

Ternary intermetallics with the composition  $R_2TM_3$ ,<sup>1-3</sup> where  $R$  is a rare earth or uranium atom,  $T$  stands for a  $d$ -electron transition metal, and  $M$  is a  $p$ -electron element, crystallize in various derivatives of the hexagonal  $AlB_2$ -type structure.<sup>4</sup> In the parent  $AlB_2$ -type unit cell, the  $R$  atoms occupy the Al positions and form triangles of nearest neighbors, while the  $T$  and  $M$  atoms are randomly distributed over the B sites into trigonal prisms of a primitive hexagonal array.<sup>3</sup> The magnetic phenomena in this family of compounds, which often have spin-glass-like character, are related not only to the topological frustration in the triangular magnetic sublattice but also to frustration of the exchange interaction between the  $R$  atoms introduced by the atomic disorder within the  $T$ -Si positions. The latter effect is a direct consequence of the fact that hybridization between the  $f$  and  $d$  electronic states strongly influences the magnetic coupling. In particular, the uranium silicides  $U_2T Si_3$  have been reported to exhibit a wide variety of magnetic behaviors that are related to the degree of atomic disorder in the  $T$ -Si sublattice.<sup>3,5</sup> Phases with the Si and  $T = Pt, Pd, \text{ or } Au$  atoms randomly distributed on the same crystallographic positions show properties characteristic of simple nonmagnetic atom-disorder spin glasses.<sup>3,6-10</sup> Alloys with partially ordered arrangements of the Si and  $T = Rh \text{ or } Ir$  atoms on the B site often exhibit ferromagnetic cluster-glass or reentrant spin-glass properties.<sup>3,5,11,12</sup> In turn, fully ordered compounds (those with  $T = Fe, Ru, \text{ and } Os$ ) do not order magnetically down to the lowest temperatures investigated.<sup>3,7,13,14</sup>

The uranium silicide  $U_2CoSi_3$ , crystallizing in the  $AlB_2$ -type structure, was initially reported to be a reentrant spin-glass system that undergoes a ferromagnetic transition at the Curie temperature of 10 K, and then exhibits spin-glass freezing at about 8 K.<sup>2</sup> In subsequent studies, performed on polycrystalline samples, the compound was characterized as a weak ferromagnet,<sup>3</sup> or a simple spin glass with strong ferromagnetic correlations.<sup>12</sup> These contradictory results motivated us to undertake a reinvestigation of this material. Here, we present the results of our comprehensive study of  $U_2CoSi_3$  performed on single-crystalline specimens. The main aim of this study was to clarify the actual nature of the electronic ground state in this compound.

## II. EXPERIMENTAL DETAILS

A single crystal of  $U_2CoSi_3$  was grown by the Czochralski pulling method in a tetra-arc furnace under an ultrapure argon atmosphere. Its crystal structure was checked by x-ray diffraction employing an Oxford Diffraction four-circle diffractometer equipped with a CCD camera, using Mo  $K\alpha$  radiation. The crystal was found to have a hexagonal structure. As no superstructure reflection was observed that would hint at enlargement of the unit cell, a simple primitive disordered  $AlB_2$ -type structure was assumed. The lattice parameters refined from the x-ray data were  $a = 3.9765(3)$  Å and  $c = 3.8980(3)$  Å, i.e., close to the values reported in the literature.<sup>2</sup> dc magnetic measurements were performed within the temperature range 1.72–400 K and in magnetic fields up to 5 T using a superconducting quantum interference device magnetometer (Quantum Design MPMS-5). ac magnetic susceptibility measurements were carried out between 3 and 9 K within the frequency range 10 Hz–10 kHz. The heat capacity was studied in the temperature interval 1–15 K and in magnetic fields up to 2 T. Temperature and magnetic field (applied perpendicular to the current flowing through the specimen) variations of the electrical resistivity were determined from 2 to 300 K in magnetic fields up to 9 T. The ac susceptibility, heat capacity, and electrical transport measurements were made using a Quantum Design PPMS-9 platform.

## III. RESULTS AND DISCUSSION

### A. dc magnetization

Figure 1 shows the temperature dependencies of the inverse magnetic susceptibility measured in an external magnetic field oriented along the  $a$  and  $c$  axes of the hexagonal unit cell. As is apparent from the plot, above about 50 K both variations follow a modified Curie-Weiss law with the parameters  $\chi_0^a = 7 \times 10^{-4}$  emu/mol,  $\mu_{\text{eff}}^a = 2.31\mu_B$ ,  $\theta_p^a = -37$  K for  $B \parallel a$ , and  $\chi_0^c = 10 \times 10^{-4}$  emu/mol,  $\mu_{\text{eff}}^c = 2.1\mu_B$ ,  $\theta_p^c = 1$  K for  $B \parallel c$ . The obtained values of  $\chi_0$  are typical for U-based intermetallics. The magnetic effective moments  $\mu_{\text{eff}}$  are smaller than those predicted for  $U^{3+}$  ( $3.62\mu_B$ ) and  $U^{4+}$  ( $3.58\mu_B$ ) free ions. The pronounced difference between the paramagnetic

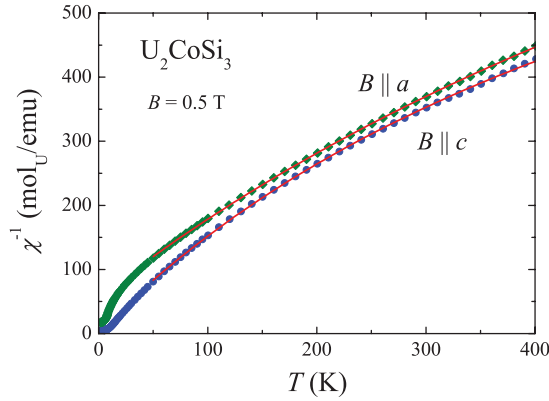


FIG. 1. (Color online) Temperature dependencies of the reciprocal molar magnetic susceptibility of  $U_2CoSi_3$  measured with magnetic field oriented along the  $a$  and  $c$  axes of the hexagonal unit cell. The solid lines represent fits of the modified Curie-Weiss law to the experimental data.

Curie temperatures  $\theta_p$  derived for the two characteristic crystallographic directions reflects magnetocrystalline anisotropy.

Figures 2(a) and 3 show the magnetization in  $U_2CoSi_3$  taken as a function of the temperature in a constant field of 0.01 T and as a function of the magnetic field strength at a fixed temperature 1.72 K, respectively. The low-temperature dependencies of the magnetization were taken in the zero-field-cooled (ZFC) and field-cooled (FC) regimes. Both figures reveal magnetocrystalline anisotropy, with the magnetization component taken along the  $c$  axis being distinctly larger than that measured along the  $a$  axis. This situation is different from that observed in similar systems  $U_2PdSi_3$  (Ref. 15) and  $U_2NiSi_3$  (Refs. 16 and 17), in which the magnetization component taken within the hexagonal plane is always larger than that taken along the  $c$  axis. The value of the magnetic transition temperature, defined as an inflection point on the  $\sigma^c(T)$  curve, amounts to 6.3 K.

The overall behavior of the low-temperature magnetization in  $U_2CoSi_3$  may suggest a ferromagnetic ground state. This is because of several features usually observed for ferromagnetically ordered systems: the variations  $\sigma_{ZFC}(T)$  and  $\sigma_{FC}(T)$  show clear bifurcations below a certain temperature, called the irreversibility temperature  $T_{ir}$ , and the  $\sigma(B)$  curves reveal hysteresis loops and significant remanence. However, the magnetic moment measured along the easy magnetization direction ( $B \parallel c$ ) at 1.72 K in a field of 5 T is rather small,  $0.35\mu_B$  (see the inset to Fig. 3), while the corresponding  $\sigma_{FC}(T)$  variation shows near 4.5 K a curvature quite unusual for regular ferromagnets, yet possible for spin-glass-like systems.<sup>18</sup> In order to get more insight into the nature of the magnetic ground state in  $U_2CoSi_3$ , the low-temperature magnetization was measured in different applied magnetic fields. The main finding was that the maximum in the ZFC variation broadens with increasing magnetic field strength, while the irreversibility temperature  $T_{ir}$  systematically shifts toward lower temperatures [see Fig. 2(b)]. The inset to Fig. 2(a) shows  $T_{ir}$  plotted as a function of  $B^{2/3}$ . The observed linear character of this variation was theoretically predicted within the mean-field model to occur in spin glasses.<sup>19</sup> Moreover, this so-called de Almeida–Thouless law was indeed reported

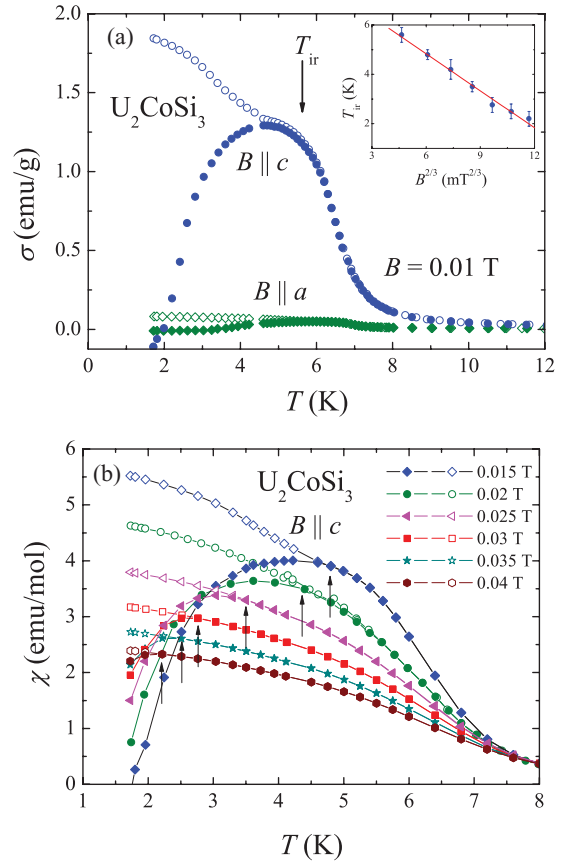


FIG. 2. (Color online) (a) Low-temperature dependencies of the magnetization in single-crystalline  $U_2CoSi_3$  measured with magnetic field oriented along two characteristic directions. Full symbols denote the data taken in the ZFC mode and open symbols refer to the data obtained in the FC regime. The inset presents the de Almeida–Thouless line, plotted as  $T_{ir}$  vs  $B^{2/3}$ . (b) Low-temperature magnetic susceptibility of  $U_2CoSi_3$  taken in different magnetic fields oriented along the  $c$  axis in ZFC (full symbols) and FC (open symbols) regimes. The arrows mark the irreversibility temperatures.

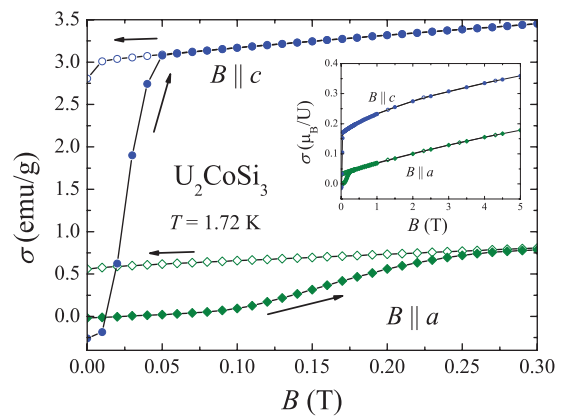


FIG. 3. (Color online) Low-field variations of the magnetization in single-crystalline  $U_2CoSi_3$  measured at  $T = 1.72$  K with magnetic field oriented parallel to the hexagonal axis. Open symbols denote the data taken with increasing field and full symbols refer to the data obtained with decreasing field. The inset presents the magnetization data up to 5 T.

before for a few other  $R_2TM_3$  compounds, such as  $U_2IrSi_3$  (Ref. 12) and  $Nd_2AgIn_3$  (Ref. 20), which were characterized in the literature as spin-glass systems. Thus, it seems reasonable to formulate a hypothesis that in  $U_2CoSi_3$  also one deals with a kind of spin-glass state in which extended short-range ferromagnetic correlations give rise to the formation of interacting magnetic clusters.

### B. ac magnetic susceptibility

In order to verify the spin-glass scenario for  $U_2CoSi_3$ , the dynamic magnetic susceptibility was studied in a field of 1 mT applied along the hexagonal  $c$  axis (the easy magnetization direction), and oscillating within the frequency range  $10 \text{ Hz} \leq \nu \leq 10 \text{ kHz}$ . As displayed in Fig. 4, the low-temperature dependencies of the real  $\chi'_{ac}$  and imaginary  $\chi''_{ac}$  components of the ac susceptibility form pronounced maxima, whose positions and amplitudes systematically shift toward higher temperatures with increasing frequency  $\nu$ . This behavior is considered as one of the main fingerprints of a spin-glass state.<sup>18,21</sup> The freezing temperature  $T_f$ , defined as a maximum in the  $\chi'_{ac}(T)$  variation, amounts to 6 K at  $\nu = 10 \text{ Hz}$ . Remarkably, this value is equal to the transition temperature evaluated from the dc magnetization data. The parameter

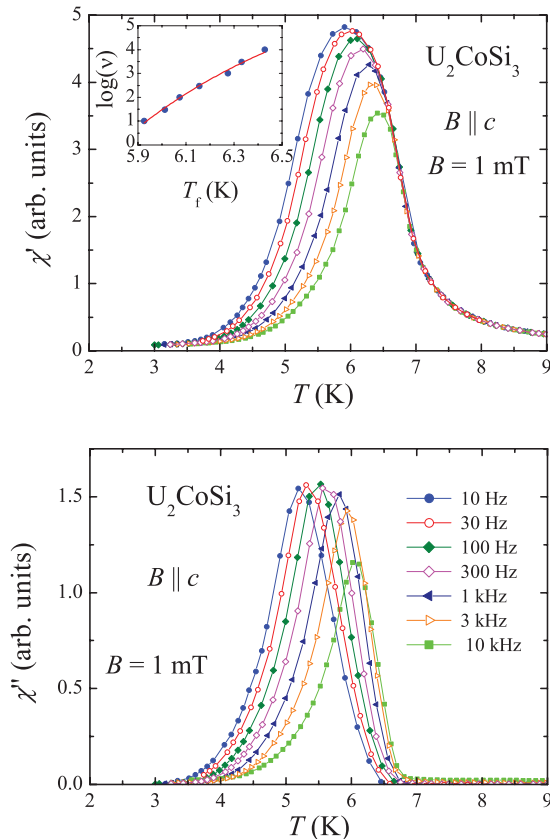


FIG. 4. (Color online) Low-temperature variations of the real and imaginary components of the ac magnetic susceptibility of single-crystalline  $U_2CoSi_3$  measured in an oscillatory field of 1 mT within the frequency range  $10 \text{ Hz} \leq \nu \leq 10 \text{ kHz}$  applied parallel to the  $c$  axis. The inset presents the correlation between the freezing temperature and the frequency of the oscillatory magnetic field. Solid line is the fit discussed in the text.

describing the relative shift of the freezing temperature,  $\delta T_f = \Delta T_f / (T_f \Delta \log_{10} \nu)$ , is often used to compare the frequency dependence of  $T_f$  in different spin glasses and spin-glass-like systems. For  $U_2CoSi_3$ ,  $\delta T_f$  is found to be 0.028, i.e., close to the values derived for other metallic spin glasses, like, e.g.,  $URh_2Ge_2$  ( $\delta T_f = 0.025$ , Ref. 21),  $U_2PdSi_3$  ( $\delta T_f = 0.02$ , Ref. 9), or  $Ce_2AgIn_3$  ( $\delta T_f = 0.022$ , Ref. 22).

For most spin glasses the frequency dependence of the freezing temperature can be properly described by the empirical Vogel-Fulcher law:<sup>18,23</sup>

$$\nu = \nu_0 \exp[-E_a / (T_f - T_0)], \quad (1)$$

where  $\nu_0$  is the characteristic frequency,  $E_a$  is the activation energy, and  $T_0$  is the Vogel-Fulcher temperature, which may be related to the true critical temperature of the phase transition for which  $T_f$  is only a dynamic manifestation.  $T_0$  might also be related to the interaction strength between the clusters in a spin glass.<sup>18,24</sup> The inset to Fig. 4 presents the relation between the frequency and the freezing temperature observed for  $U_2CoSi_3$ . The line plotted throughout experimental points is a curve given by Eq. (1) with the least-squares fitting parameters  $\nu_0 = 10^{13} \text{ Hz}$ ,  $E_a = 19 \text{ K}$ , and  $T_0 = 4.4 \text{ K}$ . Clearly, the characteristic frequency  $\nu_0$  is of the order of magnitude characteristic of spin glasses.<sup>23</sup> Moreover, the Vogel-Fulcher temperature  $T_0$  is slightly smaller than  $T_f$ , as predicted for such systems.

### C. Isothermal remanent magnetization

As a further characterization of the magnetic ground state in  $U_2CoSi_3$ , Fig. 5 shows the reduced isothermal magnetization decay measured at two different temperatures 1.72 and 2.5 K. Before each measurement the sample was first zero-field cooled from a temperature much higher than  $T_f$ , and then a magnetic field of 2 T was applied parallel to the  $c$  axis for 5 min. Afterward, the field was switched off at  $t = 0$  and the time dependence of the magnetization was recorded. As may be

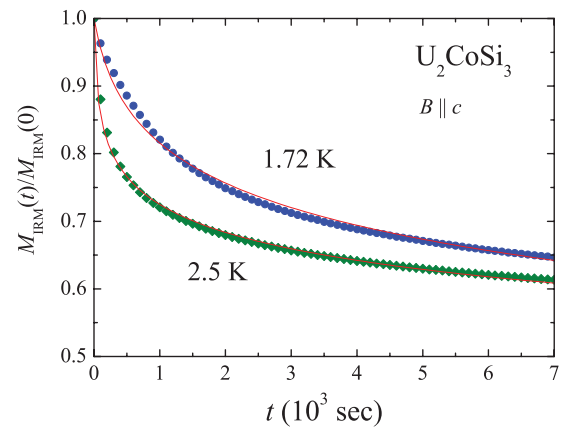


FIG. 5. (Color online) Decay of the remanent magnetization in single-crystalline  $U_2CoSi_3$  as a function of the time. The measurements were carried out at 1.72 and 2.5 K upon application of a magnetic field of 2 T along the  $c$  axis for 5 min before switching it off. The solid lines are the fits of Eq. (2) to the experimental data.

inferred from Fig. 5, the decay of the isothermal magnetization can be well represented by a logarithmic time dependence:<sup>25,26</sup>

$$M_{\text{IRM}} = M_0 + \alpha \ln \left( 1 + \frac{t}{t_0} \right), \quad (2)$$

often observed for metallic spin glasses. The parameters  $M_0$  and  $\alpha$ , called the initial zero-field magnetization and the magnetic viscosity, respectively, are temperature dependent. In turn, the coefficient  $t_0$  has only limited physical relevance and depends on experimental conditions. The least-squares fitting of the above equation to the experimental data of  $\text{U}_2\text{CoSi}_3$  yielded the following parameters:  $M_0 = 3$  emu/g,  $\alpha = -0.27$  emu/g for  $T = 1.72$  K, and  $M_0 = 0.76$  emu/g,  $\alpha = -0.05$  emu/g for  $T = 2.5$  K. These values are comparable to those reported for some other metallic spin glasses of similar type.<sup>26</sup> Such behavior of the magnetization decay is in line with other magnetic characteristics, pointing all together to the description of  $\text{U}_2\text{CoSi}_3$  as a material with spin-glass freezing.

#### D. Specific heat

Figure 6 presents the temperature variation of the specific heat of  $\text{U}_2\text{CoSi}_3$ . Remarkably, the magnetic phase transition manifests itself only as a tiny anomaly in  $C(T)$ , located slightly below the freezing temperature  $T_f$  derived from the magnetic data. This singularity involves only a very small amount of the magnetic entropy ( $0.008R \ln 2$  per U atom), which seems to be too small for the development of long-range magnetic order. On the other hand, although in canonical spin glasses the heat capacity is mostly featureless,<sup>8,10,27</sup> for systems isostructural to  $\text{U}_2\text{CoSi}_3$  and described in the literature as spin glasses with extended ferromagnetic correlations, e.g.,  $\text{U}_2\text{RhSi}_3$  and  $\text{U}_2\text{IrSi}_3$ ,<sup>11,12</sup> the reported anomalies in  $C(T)$  are very similar to that observed in the present case.

The inset to Fig. 6 shows the low-temperature specific heat data presented as  $C/T$  vs  $T^2$ . As is apparent from the plot, below  $T_f$  the heat capacity can be satisfactorily approximated by the relation  $C(T) = \gamma(0)T + \beta T^3$  with the linear specific heat coefficient  $\gamma(0)$  of  $180$  J/(mol K<sup>2</sup>). The

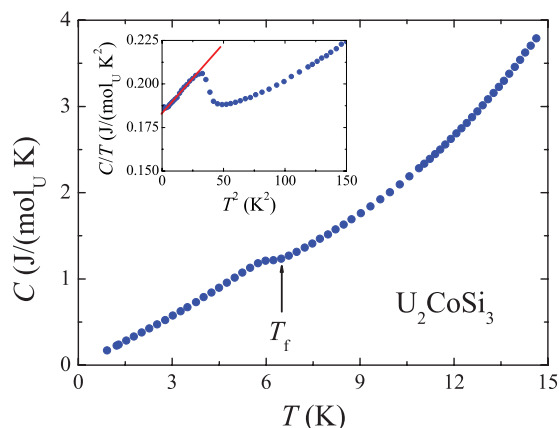


FIG. 6. (Color online) Temperature dependence of the specific heat of single-crystalline  $\text{U}_2\text{CoSi}_3$ . The freezing temperature is marked by an arrow. The inset shows the  $C/T$  vs  $T^2$  variation. Solid line emphasizes the straight-line behavior below  $T_f$ .

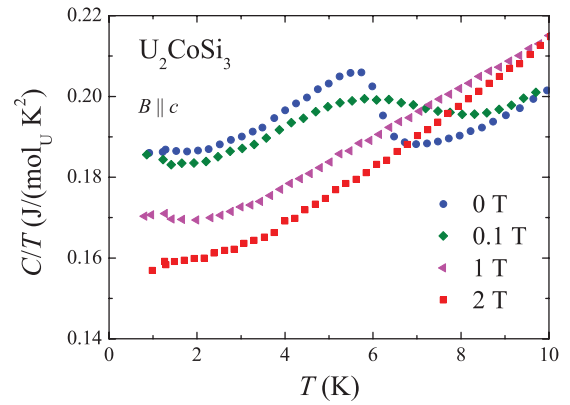


FIG. 7. (Color online) Low-temperature dependencies of the ratio of specific heat to temperature of single-crystalline  $\text{U}_2\text{CoSi}_3$ , measured in magnetic fields applied along the hexagonal  $c$  axis.

observed enhancement may be caused by both formation of heavy quasiparticles and spin-glass freezing, and these two mechanisms cannot be easily distinguished. As pointed out by Gschneidner *et al.*,<sup>28</sup> in a system with atomic disorder and/or topological frustration, an enlarged  $\gamma$  value may be a false indication of a heavy-fermion ground state.

As demonstrated in Fig. 7, upon application of an external magnetic field of 0.1 T, directed along the crystallographic  $c$  axis, the maximum in  $C/T$  vs  $T$  that is associated with the magnetic transition significantly broadens and its magnitude diminishes. In stronger magnetic fields, no anomaly in the specific heat can be recognized. The observed behavior seems fully consistent with the spin-glass scenario in  $\text{U}_2\text{CoSi}_3$ .

#### E. Electrical resistivity

The temperature dependencies of the electrical resistivity measured with the electrical current flowing along the  $a$  and  $c$  axes of the hexagonal unit cell are shown in Fig. 8. Both curves

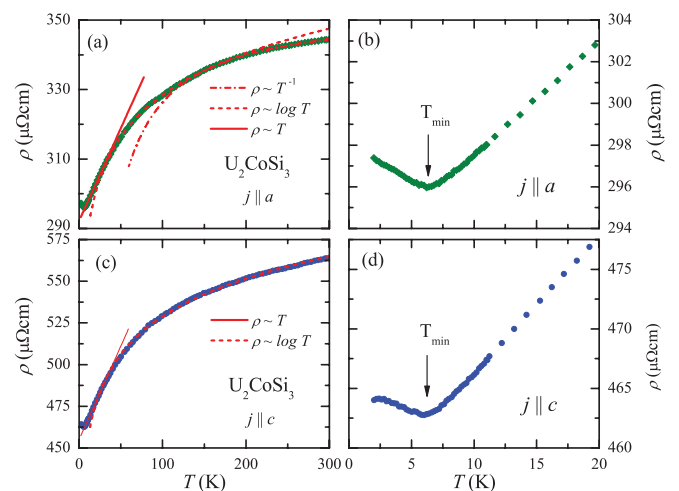


FIG. 8. (Color online) Temperature variations of the electrical resistivity of single-crystalline  $\text{U}_2\text{CoSi}_3$ , measured with the current flowing along the crystallographic  $a$  axis (upper panels) and  $c$  axis (lower panels). Solid, dashed, and dotted lines are the dependencies discussed in the text. The right-hand side panels display the low-temperature parts.

have a metalliclike character; however, the overall change in the resistivity magnitude as the temperature is decreased from 300 to 2 K is small, quantified by a residual resistivity ratio  $[\rho(300\text{ K})/\rho(2\text{ K})]$  of about 1.2 for both crystallographic directions. Remarkably, the residual resistivity itself is quite large, being equal to  $\rho^a = 297\ \mu\Omega\text{ cm}$  and  $\rho^c = 464\ \mu\Omega\text{ cm}$  for  $j \parallel a$  and  $j \parallel c$ , respectively. These features are most likely a direct consequence of the inherent atomic disorder in the Co/Si sublattice of the  $A1B_2$ -type unit cell, as revealed in the x-ray diffraction experiment.

Above 6 K, the shapes of  $\rho^a(T)$  and  $\rho^c(T)$  are reminiscent of the behavior known for metals in which the electrical transport is governed by strong local spin fluctuations. In such systems, one may expect at low temperatures a  $T^2$  dependence of  $\rho(T)$ , which is followed by a range of a linear behavior and then replaced by a logarithmic variation  $\rho \propto \log T$  above the so-called spin fluctuation temperature  $T_{\text{sf}}$ .<sup>29–31</sup> At high temperatures, the resistivity is expected to approach a spin disorder (unitarity) limit changing with the temperature as  $\rho \propto [1 - (T_{\text{sf}}/T)]$ . As may be inferred from Fig. 8, rather extended regions of the subsequent linear, logarithmic, and hyperbolic temperature dependencies of the resistivity can be identified in the data collected for  $j \parallel a$ . In the  $\rho^c(T)$  curve, the  $\rho \propto T^{-1}$  variation cannot be discerned, yet the other two are clearly seen. In turn, in neither of the two principal directions is the low-temperature  $T^2$  dependence observed, and this is because of the appearance of distinct resistivity minima at 6 K [see Figs. 8(b) and 8(d)]. These anomalies clearly coincide with those observed in the magnetic and specific heat data at the freezing temperature  $T_f$ . It is worthwhile to recall that a fairly similar minimum in the electrical resistivity was previously observed in  $\text{U}_2\text{IrSi}_3$ , where it was attributed to the formation of a ferromagnetic cluster-glass state.<sup>12</sup> However, it should be stressed that, below the respective  $T_f$ , the resistivity in neither  $\text{U}_2\text{IrSi}_3$  nor  $\text{U}_2\text{CoSi}_3$  exhibits  $\rho \propto T^{3/2}$  or  $\rho \propto T^2$  variations, predicted theoretically for spin glasses.<sup>32,33</sup> In turn, a different interpretation of the occurrence of low-temperature minima in  $\rho(T)$  was given for a few other members of the  $\text{U}_2T\text{Si}_3$  family; namely, for the phases with  $T = \text{Pd, Pt, and Au}$  this feature was considered as a hallmark of the Kondo effect.<sup>9</sup> However, in contrast to the present case of  $\text{U}_2\text{CoSi}_3$ , the observed resistivity minima were broad and located at a temperature twice  $T_f$  as determined from the magnetic data.

In order to evaluate the concept of the Kondo effect in more detail, the low-temperature electrical resistivity of  $\text{U}_2\text{CoSi}_3$  was measured in applied magnetic fields. The obtained experimental data are plotted in Fig. 9. For  $j \parallel a$  and  $B \parallel c$ , a magnetic field of 1 T reduces the minimum from 0.5% to 0.25%, while the temperature of the minimum remains almost unaltered. In stronger magnetic fields, the minimum in  $\rho^a(T)$  becomes deeper and gradually shifts toward higher temperatures (see the reduced resistivity plot in the upper right-hand side panel in Fig. 9). Remarkably, for  $B \geq 1\text{ T}$ , the ratio  $(\Delta\rho/\rho_{2\text{ K}})^a$  is proportional to  $-AT^{1/2}$  with roughly independent of the magnetic field strength  $A = 0.85\ \mu\Omega\text{ cm K}^{0.5}$ . Such behavior rules out the dominant role of the Kondo effect for which an upturn in  $\rho(T)$  is expected to be proportional to  $\log T$ , while its magnitude should be diminished by a magnetic field, giving thus a negative contribution to the total magnetoresistivity. Additionally, the Kondo minimum is

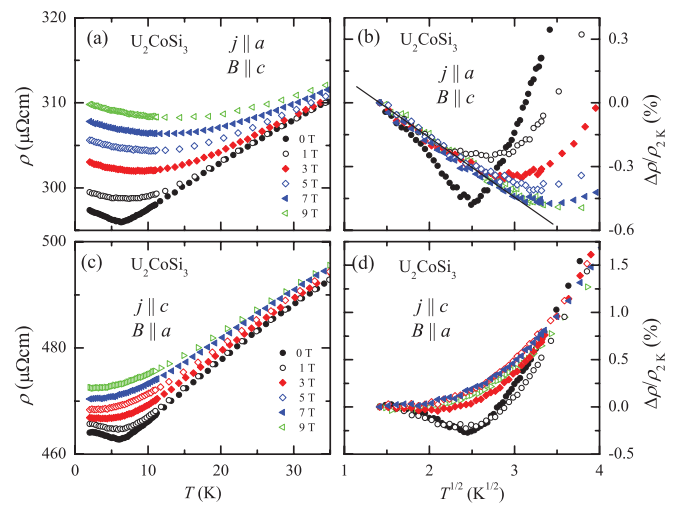


FIG. 9. (Color online) Left-hand panels: low-temperature dependencies of the electrical resistivity of single-crystalline  $\text{U}_2\text{CoSi}_3$ , measured along the crystallographic  $a$  axis (upper panels) and  $c$  axis (lower panels) in external magnetic field applied along the  $c$  and  $a$  axes, respectively. Right-hand panels: relative change of the electrical resistivity of  $\text{U}_2\text{CoSi}_3$ , measured as in the other panels, plotted as a function of square root of the temperature.

expected to move toward lower temperatures with increasing magnetic field strength, and just the opposite effect is seen in  $\rho^a(T)$  of  $\text{U}_2\text{CoSi}_3$ . In the case of the resistivity measured along the  $c$  axis, the observed minimum is only half that in  $\rho^a(T)$ , and application of magnetic fields stronger than 3 T leads to a rapid suppression of this anomaly (see the lower panels in Fig. 9). Alike, for the other current configuration, the magnetoresistance is positive in the low-temperature region.

The observed upturn in the electrical resistivity might be considered to be a result of some other physical phenomena. One of them is the presence of critical spin fluctuations in the vicinity of the antiferromagnetic phase transition. However, in such a case the magnetoresistivity measured in the critical region is negative,<sup>34,35</sup> which contrasts with the behavior established for  $\text{U}_2\text{CoSi}_3$ . Another mechanism relates the increase of the electrical resistivity with decreasing temperature to the formation of magnetic superzone gaps in the ordered phase.<sup>36</sup> This latter scenario seems also not applicable the case of  $\text{U}_2\text{CoSi}_3$ , which is a spin-glass system and thus the occurrence of a magnetic superzone gap seems unlikely.

The presence of strong atomic disorder in  $\text{U}_2\text{CoSi}_3$  raises a question of a possible description of the low-temperature behavior of its electrical resistivity in terms of theories developed for disordered conductors, which involve quantum corrections to the conductivity, such as electron-electron interaction (EEI) and weak localization (WL) effects.<sup>37,38</sup> Indeed, both these mechanisms give rise to the formation of some minima in  $\rho(T)$ . Within the WL scenario, the extra contribution to the resistivity due to the quantum interference effect is of the type  $\Delta\rho_{\text{WL}} \propto -T^{n/2}$ , where  $n \geq 1.5$ , which is different from the behavior observed for  $\text{U}_2\text{CoSi}_3$ . The conjecture of a quantum interference effect in the electrical resistivity was earlier formulated for a few uranium compounds.<sup>39,40</sup> Moreover, the description of the electrical resistivity in terms of the weak localization effect has been applied, for example,

to  $\text{HoMn}_{12-x}\text{Fe}_x$ .<sup>41</sup> In the latter case the electrical resistivity increase below  $T_N$  was shown to be mainly due to reduction in the elastic mean free path  $l_{\text{dis}}^e$ , limited by substitutional spin-disorder scattering. However, if the reduction of  $l_{\text{dis}}^e$  with decreasing temperature is a dominating mechanism leading to the increase of the dephasing length scale  $1/L_\varphi$ , the relation  $1/l_{\text{dis}}^e \propto T^{3/2}$  implies that the correction to the conductivity due to weak localization is of the form  $\Delta\rho_{\text{WL}} \propto 1/L_\varphi \propto T^{3/2}$ . In turn, according to the theoretical prediction by Altshuler and Aronov,<sup>38</sup> the correction to the resistivity is proportional to  $-T^{1/2}$ . Remarkably, the experimental data for  $\Delta\rho^a/\rho^a(2\text{ K})$  (compare Fig. 9) follow the  $-T^{1/2}$  behavior, hence suggesting that the low-temperature upturn in  $\rho^a(T)$  is likely mainly governed by the electron-electron interactions. The minimum in  $\rho^a(T)$  which shifts to higher temperatures upon applying magnetic field is also in accordance with the EEI theory. In this case the resulting magnetoresistivity which arises from the Zeeman effect is positive and increases with increasing ratio  $g\mu_B B/k_B T$ .

The transverse magnetoresistivity  $\Delta\rho/\rho$  data ( $\Delta\rho/\rho = \frac{\rho(B) - \rho(B=0)}{\rho(B=0)}$ ) for the current flowing along the crystallographic  $a$  and  $c$  axes are shown in Fig. 10. As mentioned above, the values of  $\Delta\rho/\rho$ , both above and below  $T_f$ , are positive and increase monotonically with increasing magnetic field strength. For both directions, the largest magnitude of  $\Delta\rho/\rho$  is obtained at 6 K. In  $B = 9\text{ T}$ ,  $\Delta\rho/\rho$  measured for  $j \parallel a$  and  $B \parallel c$  is twice that obtained for  $j \parallel c$  and  $B \parallel a$ . Remarkably, in fairly extended magnetic field strength intervals, especially at low temperatures and for  $j \parallel a$ , the magnetoresistivity is proportional to  $B^{1/2}$  (see Fig. 10). It is also worth noting that above  $T_f$  the magnitude of  $\Delta\rho/\rho$  decreases with increasing temperature, and the field range of the  $\Delta\rho/\rho \sim B^{1/2}$  dependence is reduced.

The  $\Delta\rho/\rho$  behavior observed for  $\text{U}_2\text{CoSi}_3$  is very similar to that predicted for disordered metals, in which the

electronic transport is influenced by quantum corrections.<sup>42–44</sup> According to the WL theory, in the presence of strong spin-orbit interactions such that  $B_\varphi \ll B_{\text{so}}$  ( $B_{\varphi,\text{so}} = \hbar/4eD\tau_{\varphi,\text{so}}$ , where  $\tau_{\varphi,\text{so}}$  stands for the dephasing and spin-orbit relaxation time, respectively, and  $D$  is a diffusion coefficient), the transverse magnetoresistivity should be positive and vary as  $B^{1/2}$  in the strong field limit. Square-root behavior of the magnetoresistivity at sufficiently high fields such that  $g_{\text{eff}}\mu_B B/k_B T \gg 1$  ( $g_{\text{eff}}$  is an effective Landé factor that accounts for spin fluctuations) is also predicted for EEI in disordered solids. Usually, the influence of a magnetic field on the interaction effects is less than on the quantum correction to the resistivity of a noninteracting electron gas. This is particularly true if one takes into account the presence of spin-orbit interaction, because the magnetic scattering mixes spin-up and spin-down subbands and it is required that  $g_{\text{eff}}\mu_B B \gg \hbar/\tau_{\text{so}}$  in order to observe the magnetoresistivity due to the Zeeman spin-splitting effect. On the other hand, the presence of spin fluctuations strengthens the Zeeman effect by increasing  $g_{\text{eff}}$ . The effect of different contributions to the magnetoresistivity of  $\text{U}_2\text{CoSi}_3$  may be inferred from the  $\Delta\rho/\rho(B)$  variation measured at 2 K with the current  $j \parallel c$  (Fig. 10). It seems that two inflection points occurring on this  $\Delta\rho/\rho$  isotherm at 3 and 6.5 T can be associated with two different characteristic magnetic field scales. In contrast, the magnetoresistivity measured with the current flowing along the  $a$  axis does not show similar features. The magnitude of  $\Delta\rho/\rho$  taken in this direction is much larger than that measured along the  $c$  axis, which presumably indicates predominance of WL in the presence of strong spin-orbit interaction.

Interestingly, the temperature at which the maximum in the magnetoresistivity is observed coincides with the minimum in  $\rho(T)$  for both orientations of the magnetic fields with respect to the crystallographic direction. Usually, in terms of the WL approach (in the presence of strong spin-orbit interactions) one may expect that the magnetoresistivity increases with decreasing temperature, because of reduction in the characteristic field  $B_\varphi$ . In the case of  $\text{U}_2\text{CoSi}_3$  such behavior is not observed below  $T_f$ . This finding can be rationalized by considering some influence of the spin fluctuations on the quantum correction, the amplitude of which takes its maximum value just at the magnetic transition. It is known that the spin fluctuation contribution may significantly increase the magnetoresistivity for both the WL and EEI scenarios, since it enlarges the splitting between spin subbands. Moreover, in the presence of spin fluctuations the electron-electron interaction constant  $F$  can be greater than 1 (due to the Stoner enhancement factor), and hence the triplet term  $(3/2)F$  can be larger than the singlet  $4/3$  component in the EEI correction to the resistivity.<sup>45–47</sup> Then, under such conditions, no minimum in  $\rho(T)$  would be observed. On the other hand, one may expect that below  $T_f$  the amplitude of spin fluctuations diminishes significantly. This implies strong reduction in the value of  $F$ , such that  $4/3 > (3/2)F$  and the minimum in  $\rho(T)$  should occur.

#### IV. SUMMARY

The results of our comprehensive studies of single-crystalline  $\text{U}_2\text{CoSi}_3$  by means of dc and ac magnetic susceptibility, heat capacity, electrical resistivity, and

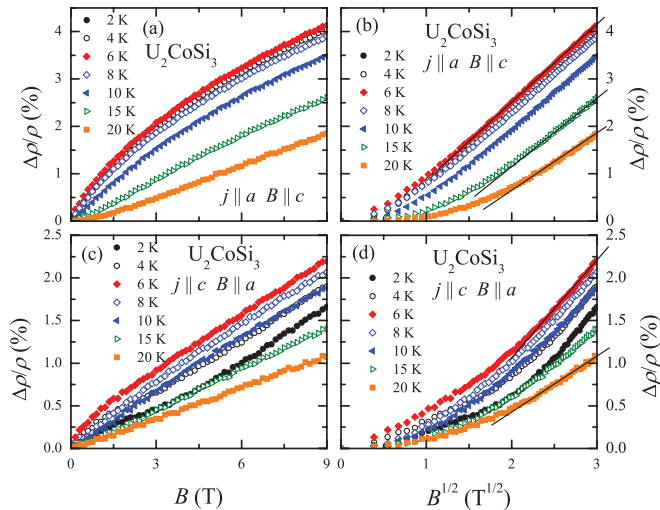


FIG. 10. (Color online) Transverse magnetoresistivity isotherms of single-crystalline  $\text{U}_2\text{CoSi}_3$  taken at several different temperatures with the current flowing along the crystallographic  $a$  axis (upper panels) and  $c$  axis (lower panels) in external magnetic field applied along the  $c$  and  $a$  axes, respectively. The right-hand panels display the  $\Delta\rho/\rho$  data as a function of the square root of the field strength. Solid lines emphasize quasilinear behavior.

magnetoresistivity measurements, performed in wide ranges of temperature and magnetic field strength, strongly suggest the formation at low temperatures of a cluster-glass state. The irreversibility in the FC and ZFC magnetization, observed below the freezing temperature  $T_f$  of 6 K, can be described by the de Almeida–Thouless law. The value of  $T_f$ , obtained from the ac susceptibility data, was found to rise with increasing frequency of the oscillatory magnetic field, in a manner characteristic of spin glasses. On the other hand, the dc magnetization indicated the presence of strong short-range ferromagnetic interactions, and therefore it seems likely that  $U_2CoSi_3$  is a ferromagnetic cluster-glass material. The cluster-glass scenario seems further supported by the heat capacity and the electrical resistivity data. The freezing effect manifests itself on the  $C(T)$  curve as a tiny anomaly just below  $T_f$ , unlike the phase transition in a long-range-ordered system but also at odds with the typical behavior in simple spin glasses. Moreover, the low-temperature electrical resistivity does not follow a  $T^{2/3}$  or  $T^2$  dependency, that would be expected for spin-glass systems.<sup>8,9,11,12</sup> Instead, the  $\rho(T)$  curves are dominated by pronounced minima which can be well described in terms of the theories appropriate for structurally disordered metals. Also the behavior of the transverse magnetoresistance is different from that expected for ferromagnets and spin glasses, yet compatible with transport scenarios involving enhanced electron-electron interactions and weak-localization effects.

Despite the absence of clear features in the behavior of  $U_2CoSi_3$  that might indicate the formation of a long-range

magnetically ordered state, the latter cannot be entirely ruled out at the present stage of the study. Here, it is worthwhile to recall the case of  $U_2NiSi_3$ , a close counterpart to  $U_2CoSi_3$ , which exhibits similar properties in the bulk magnetic measurements and shows hardly any anomaly in the heat capacity. Nevertheless, neutron diffraction experiments unambiguously revealed a ferromagnetic order that coexists with the cluster-glass state.<sup>17</sup> Obviously, the actual nature of the magnetic ground state in  $U_2CoSi_3$  should also be verified by means of neutron scattering.

Finally, it should be noted that the freezing temperature obtained for single-crystalline  $U_2CoSi_3$  is smaller than that presented in the literature.<sup>2</sup> Moreover, contrary to the previous reports,<sup>2,3</sup> no separate ferromagnetic phase transition was found above  $T_f$ . These discrepancies with the literature data may be rationalized by assuming pronounced sensitivity of the magnetic properties to some deviations from the ideal stoichiometry, which likely affected the properties of the polycrystalline samples studied before,<sup>3,8,9,48</sup> as found for a few related  $R_2TM_3$  intermetallics.

#### ACKNOWLEDGMENTS

The authors are grateful to L. Gulay for his assistance in growing the  $U_2CoSi_3$  single crystal and J. Stepien-Damm for orienting it on a four-circle diffractometer. This work was supported by the Ministry of Science and Higher Education within the Research Project No. N N202 126436.

\*d.kaczorowski@int.pan.wroc.pl

<sup>1</sup>R. Pöttgen and D. Kaczorowski, *J. Alloys Compd.* **201**, 157 (1993).

<sup>2</sup>D. Kaczorowski and H. Noël, *J. Phys.: Condens. Matter* **5**, 9185 (1993).

<sup>3</sup>B. Chevalier, R. Pöttgen, B. Darriet, P. Gravereau, and J. Etourneau, *J. Alloys Compd.* **233**, 150 (1996).

<sup>4</sup>R.-D. Hoffmann and R. Pöttgen, *Z. Kristallogr.* **216**, 127 (2001).

<sup>5</sup>K. Yubuta, T. Yamamura, and Y. Shiokawa, *J. Phys.: Condens. Matter* **18**, 6109 (2006).

<sup>6</sup>C. Geibel, C. Kämmerer, E. Göring, G. Sparr, R. Henseleit, G. Cordier, S. Horn, and F. Steglich, *J. Magn. Magn. Mater.* **90-91**, 435 (1990).

<sup>7</sup>T. Yamamura, D. Li, K. Yubuta, and Y. Shiokawa, *J. Alloys Compd.* **408-412**, 1324 (2006).

<sup>8</sup>D. Li, Y. Shiokawa, Y. Homma, A. Uesawa, A. Dönni, T. Suzuki, Y. Haga, E. Yamamoto, T. Honma, and Y. Ōnuki, *Phys. Rev. B* **57**, 7434 (1998).

<sup>9</sup>D. X. Li, Y. Shiokawa, Y. Haga, E. Yamamoto, and Y. Ōnuki, *J. Phys. Soc. Jpn.* **71**, 418 (2002).

<sup>10</sup>D. Li, A. Kimura, Y. Homma, Y. Shiokawa, A. Uesawa, and T. Suzuki, *Solid State Commun.* **108**, 863 (1998).

<sup>11</sup>D. Li, A. Dönni, Y. Kimura, Y. Shiokawa, Y. Homma, E. Y. Y. Haga, T. Honma, and Y. Ōnuki, *J. Phys.: Condens. Matter* **11**, 8263 (1999).

<sup>12</sup>D. X. Li, S. Nimori, Y. Shiokawa, Y. Haga, E. Yamamoto, and Y. Ōnuki, *Phys. Rev. B* **68**, 172405 (2003).

<sup>13</sup>N. Takeda and M. Ishikawa, *J. Phys. Soc. Jpn.* **67**, 1062 (1998).

<sup>14</sup>R. Pöttgen, P. Gravereau, B. Darriet, B. Chevalier, E. Hickey, and J. Etourneau, *J. Mater. Chem.* **4**, 463 (1994).

<sup>15</sup>D. X. Li, A. Kimura, Y. Haga, S. Nimori, and T. Shikama, *J. Phys.: Condens. Matter* **23**, 076003 (2011).

<sup>16</sup>A. Schröder, M. F. Collins, C. V. Stager, J. D. Garret, J. E. Greedan, and Z. Tun, *J. Magn. Magn. Mater.* **140-144**, 1407 (1995).

<sup>17</sup>M. Szlawska, D. Kaczorowski, and M. Reehuis, *Phys. Rev. B* **81**, 094423 (2010).

<sup>18</sup>J. A. Mydosh, *Spin Glasses: An Experimental Introduction* (Taylor & Francis, London, 1993).

<sup>19</sup>J. R. L. de Almeida and D. J. Thouless, *J. Phys. A* **11**, 983 (1978).

<sup>20</sup>D. Li, S. Nimori, Y. Shiokawa, A. Tobo, H. Onodera, Y. Haga, E. Yamamoto, and Y. Ōnuki, *Appl. Phys. Lett.* **79**, 4183 (2001).

<sup>21</sup>S. Süllow, G. J. Nieuwenhuys, A. A. Menovsky, J. A. Mydosh, S. A. M. Mentink, T. E. Mason, and W. J. L. Buyers, *Phys. Rev. Lett.* **78**, 354 (1997).

<sup>22</sup>T. Nishioka, Y. Tabata, T. Taniguchi, and Y. Miyako, *J. Phys. Soc. Jpn.* **69**, 1012 (2000).

<sup>23</sup>J. L. Tholence, *Solid State Commun.* **35**, 113 (1980).

<sup>24</sup>S. Shtrickman and E. P. Wohlfarth, *Phys. Lett. A* **85**, 467 (1981).

<sup>25</sup>S. Majumdar, E. V. Sampathkumaran, D. Eckert, A. Handstein, K.-H. Müller, S. R. Saha, H. Sugawara, and H. Sato, *J. Phys.: Condens. Matter* **11**, L329 (1999).

<sup>26</sup>D. X. Li, S. Nimori, Y. Shiokawa, Y. Haga, E. Yamamoto, and Y. Ōnuki, *Phys. Rev. B* **68**, 012413 (2003).

- <sup>27</sup>D. Li, T. Yamamura, S. Nimori, K. Yubuta, and Y. Shiokawa, *Appl. Phys. Lett.* **87**, 142505 (2005).
- <sup>28</sup>K. A. Gschneidner, J. Tang, S. K. Dhar, and A. Goldman, *Physica B* **163**, 507 (1990).
- <sup>29</sup>A. Kaiser and S. Doniach, *Int. J. Magn.* **1**, 11 (1970).
- <sup>30</sup>N. Rivier and V. Zlatic, *J. Phys. F* **2**, 99 (1972).
- <sup>31</sup>N. Rivier and V. Zlatic, *J. Phys. F* **2**, 87 (1972).
- <sup>32</sup>N. Rivier and K. Atkins, *J. Phys. F* **5**, 1745 (1975).
- <sup>33</sup>I. A. Campbell, P. J. Ford, and A. Hamzić, *Phys. Rev. B* **26**, 5195 (1982).
- <sup>34</sup>S. Alexander, J. Helman, and I. Balberg, *Phys. Rev. B* **13**, 304 (1976).
- <sup>35</sup>I. Balberg and J. S. Helman, *Phys. Rev. B* **18**, 303 (1978).
- <sup>36</sup>M. Ellerby, K. A. McEwen, and J. Jensen, *Phys. Rev. B* **57**, 024457 (1998).
- <sup>37</sup>E. Abrahams, P. W. Anderson, D. C. Licciardello, and T. V. Ramakrishnan, *Phys. Rev. Lett.* **42**, 673 (1979).
- <sup>38</sup>B. L. Altshuler and A. G. Aronov, *Sov. Phys. JETP* **50**, 968 (1979).
- <sup>39</sup>A. Otop, S. Süllow, M. B. Maple, A. Weber, E. W. Scheidt, T. J. Gortenmulder, and J. A. Mydosh, *Phys. Rev. B* **72**, 024457 (2005).
- <sup>40</sup>S. Süllow, S. A. M. Mentink, T. E. Mason, R. Feyerherm, G. J. Nieuwenhuys, A. A. Menovsky, and J. A. Mydosh, *Phys. Rev. B* **61**, 8878 (2000).
- <sup>41</sup>J. Stankiewicz, J. Bartolomé, and D. Fruchart, *Phys. Rev. Lett.* **89**, 106602 (2002).
- <sup>42</sup>H. Fukuyama and K. Hoshino, *J. Phys. Soc. Jpn.* **50**, 2131 (1981).
- <sup>43</sup>P. A. Lee and T. V. Ramakrishnan, *Phys. Rev. B* **26**, 4009 (1982).
- <sup>44</sup>B. L. Altshuler, A. G. Aronov, A. I. Larkin, and D. E. Khmel'nitskii, *Sov. Phys. JETP* **54**, 411 (1981).
- <sup>45</sup>A. J. Millis and P. A. Lee, *Phys. Rev. B* **30**, 6170 (1984).
- <sup>46</sup>M. L. Trudeau and R. W. Cochrane, *Phys. Rev. B* **38**, 5353 (1988).
- <sup>47</sup>M. Olivier, J. O. Strom-Olsen, and Z. Altounian, *Phys. Rev. B* **35**, 333 (1987).
- <sup>48</sup>D. P. Rojas, J. Rodríguez Fernández, J. I. Espeso, J. C. Gómez Sal, J. C. da Silva, F. G. Gandra, A. O. dos Santos, and A. N. Medina, *J. Magn. Magn. Mater.* **322**, 3192 (2010).